

## SUPPORTING INFORMATION

### Halogen-substituted Fullerene Derivatives for Interface Engineering in Perovskite Solar Cells

Hui Wang<sup>1,2</sup>, Feilong Cai<sup>1,2</sup>, Meng Zhang<sup>3</sup>, Pang Wang<sup>1,2</sup>, Jiaxu Yao<sup>1,2</sup>, Robert S. Gurney<sup>1,2</sup>,  
Fabao Li<sup>3</sup>, Dan Liu<sup>1,2</sup>, Tao Wang<sup>1,2\*</sup>

<sup>1</sup>State Key Laboratory of Silicate Materials for Architectures, Wuhan University of Technology,  
Wuhan, 430070, China

<sup>2</sup>School of Materials Science and Engineering, Wuhan University of Technology, Wuhan, 430070,  
China \* E-mail: twang@whut.edu.cn

<sup>3</sup>School of Chemistry and Chemical Engineering, Hubei University, Wuhan 430062, China

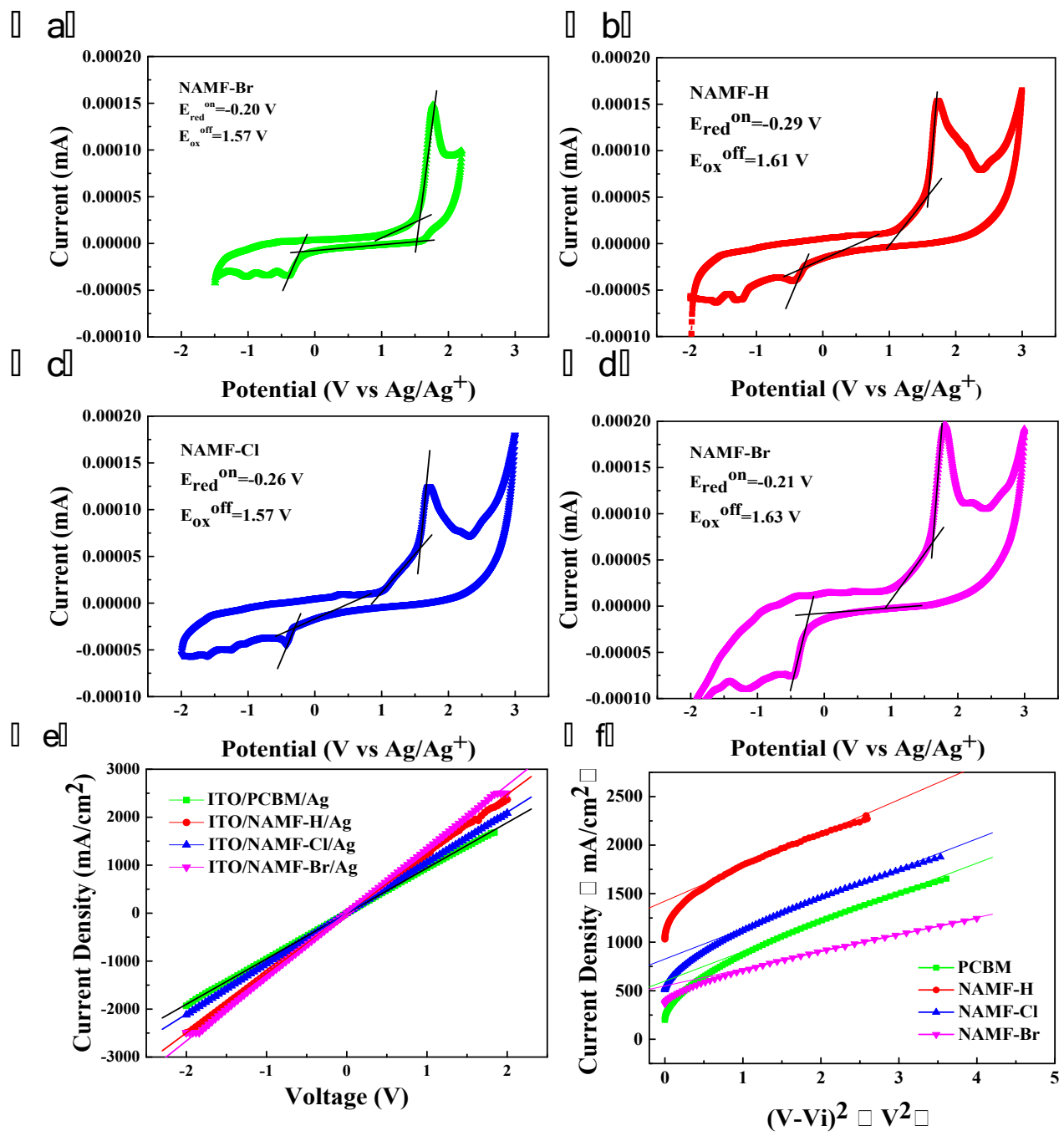


**Fig. S1.** Cyclic voltammograms of (a) PCBM, (b) NAMF-H, (c) NAMF-Cl and (d) NAMF-Br films. The dark  $J-V$  curves to calculate (e) conductivity and (f) mobility of fullerene derivatives.

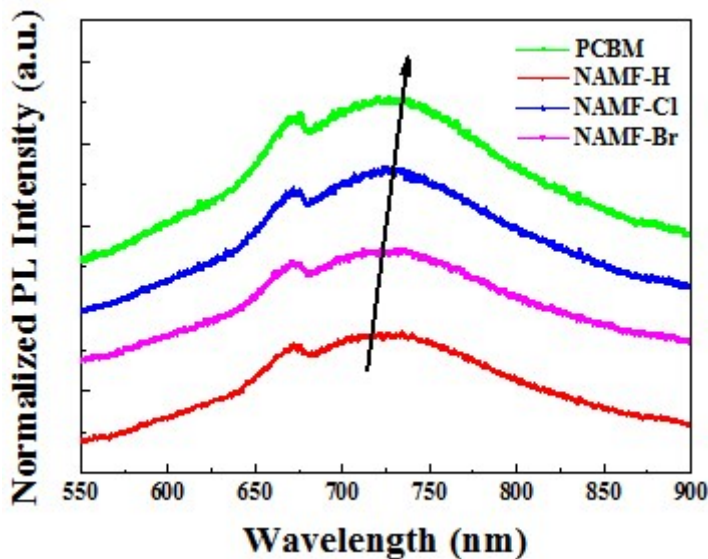


**Fig. S2.** The PL spectra of thin films of different fullerene derivatives.

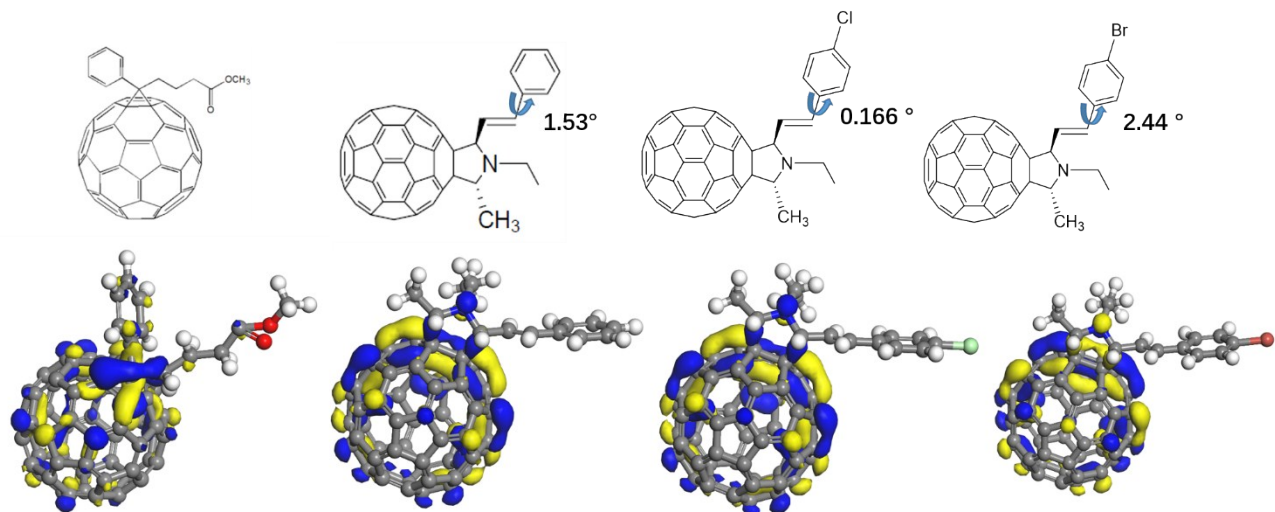


**Fig. S3.** Computed orbit profiles of NAMF-H, NAMF-Cl, NAMF-Br and PCB. Quantitative values of LUMO orbit and dihedral angle are in arbitrary unit.

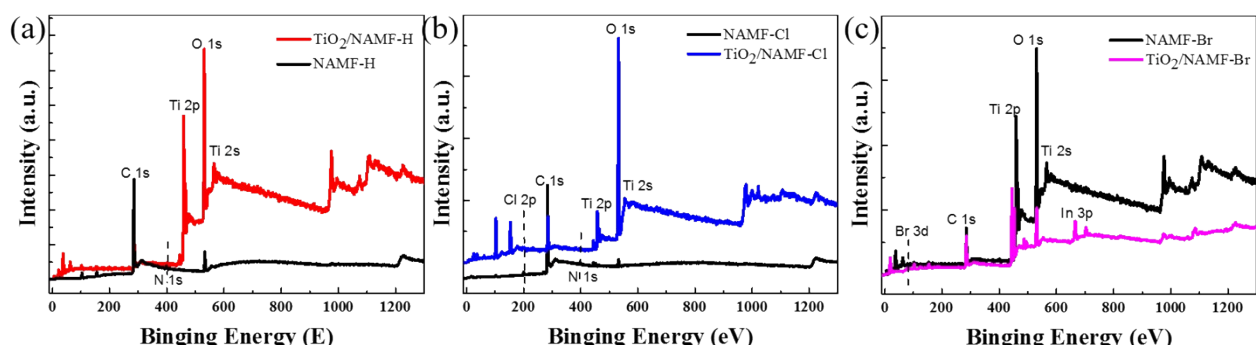


**Fig. S4.** (a-c) XPS spectra of the fullerene derivatives and  $\text{TiO}_2$ /fullerene derivative bilayers.

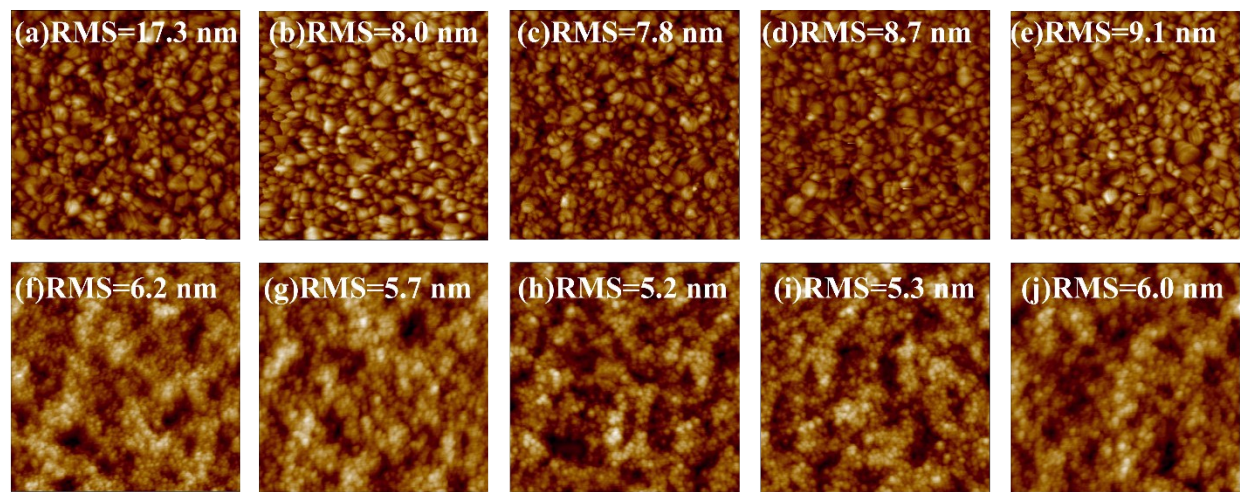


**Figure S5.** Images from scanning probe microscope (SPM) showing the surface morphology for (a) TiO<sub>2</sub>/perovskite, (b) TiO<sub>2</sub>/PCBM/perovskite, (c) TiO<sub>2</sub>/NAMF-H/perovskite, (d) TiO<sub>2</sub>/NAMF-Cl/perovskite, (e) TiO<sub>2</sub>/NAMF-Br/perovskite, (f) TiO<sub>2</sub>, (g) TiO<sub>2</sub>/PCBM, (h) TiO<sub>2</sub>/NAMF-H, (i) TiO<sub>2</sub>/NAMF-Cl and (j) TiO<sub>2</sub>/NAMF-Br/perovskite.

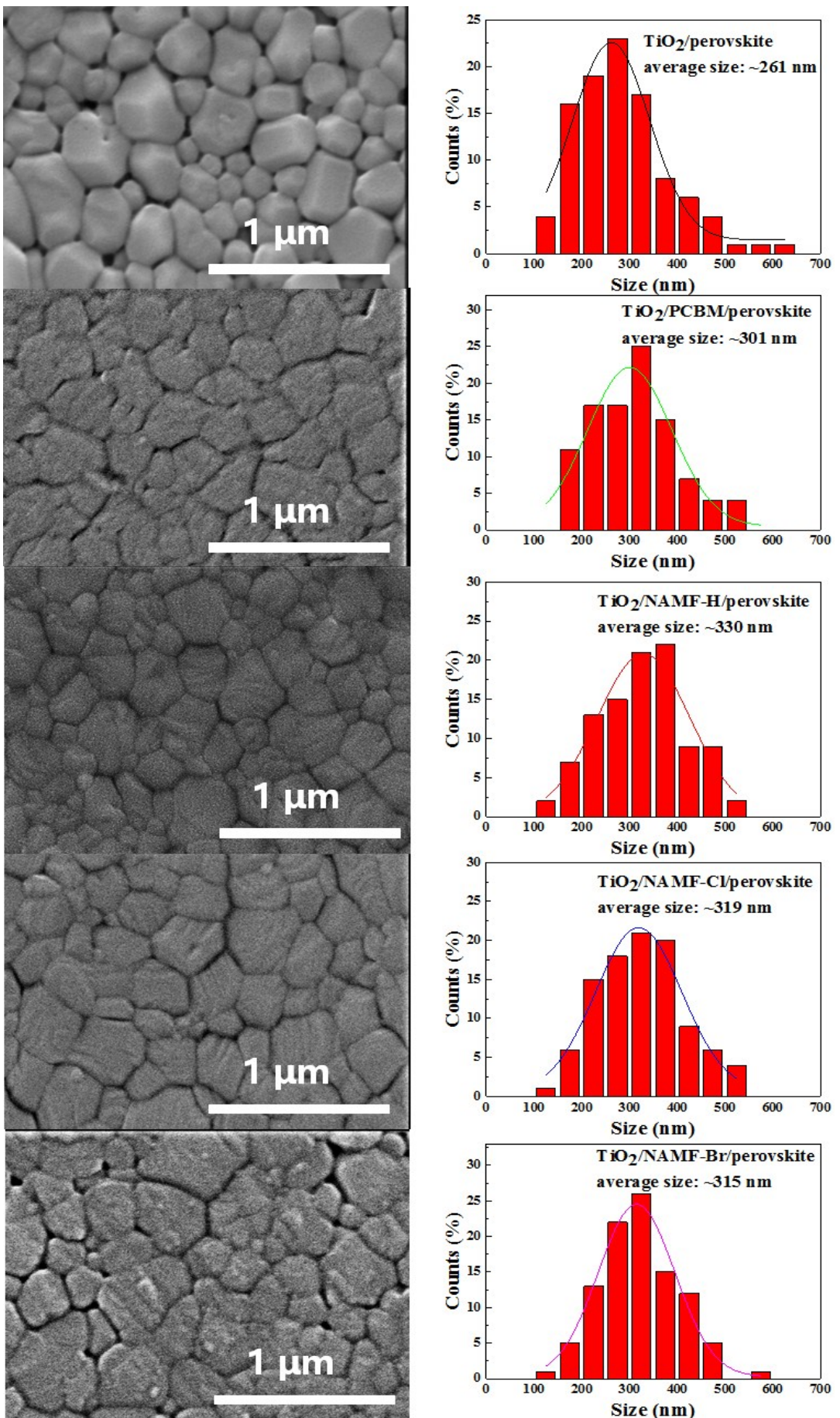


**Fig. S6.** SEM images of perovskite films cast on different fullerene derivative surfaces: (a) pure TiO<sub>2</sub>; (b) TiO<sub>2</sub>/PCBM; (c) TiO<sub>2</sub>/NAMF-H; (d) TiO<sub>2</sub>/NAMF-Cl; (e) TiO<sub>2</sub>/NAMF-Br.

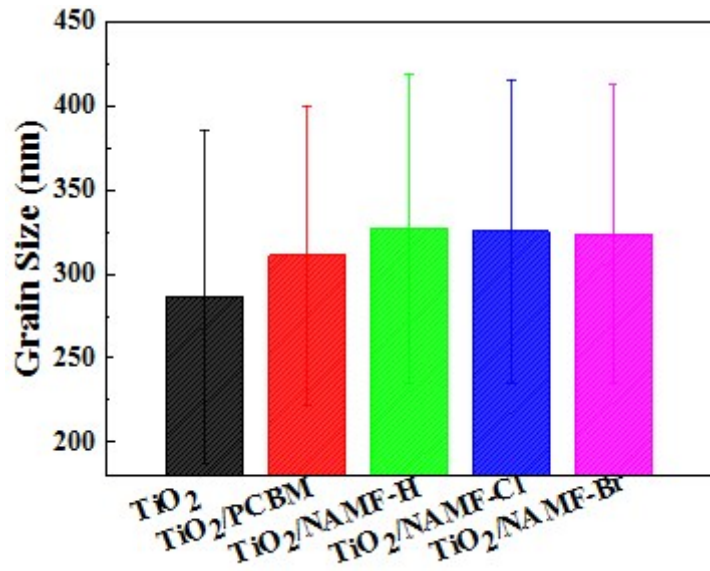


**Fig. S7.** Grain size evaluation of  $\text{MAPbI}_3$  cast on different fullerene interlayers from SEM surface images: The histogram represents the mean value, and the error bar stands for the standard deviation.

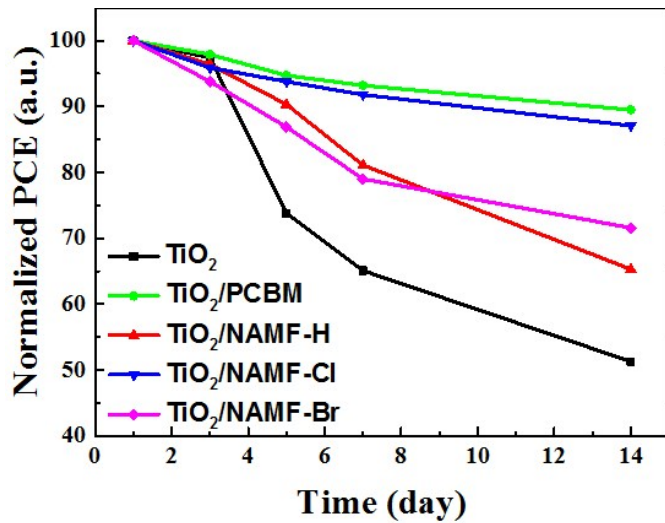


**Fig. S8.** The evolution of device PCE obtained by storing unencapsulated devices in ambient conditions having a relative humidity of  $40 \pm 5\%$  and an average temperature of  $25^\circ\text{C}$ .

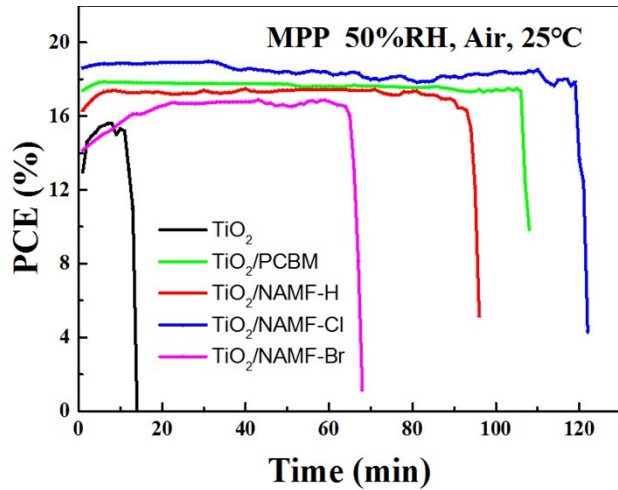


**Fig. S9.** Operational lifetimes of PSCs at the maximum power point (MPP) and ambient condition.

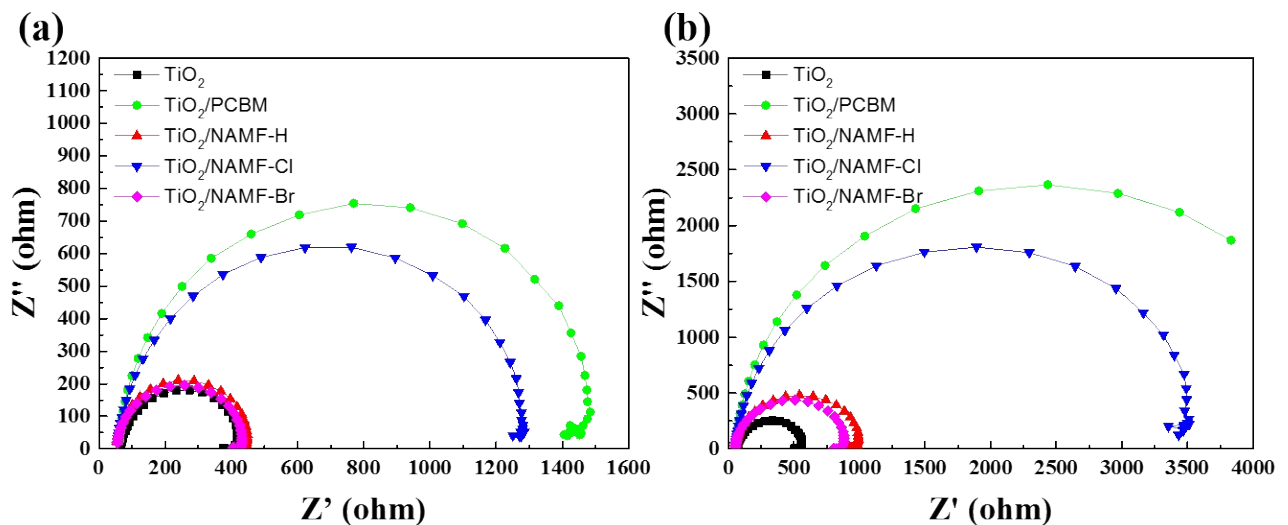


**Figure S10.** Electrochemical impedance spectroscopy (EIS) measurements. Nyquist plots for the PSCs with and without fullerene derivative interlayers at an applied bias of (a) 0.8V and (b) 0.2V.

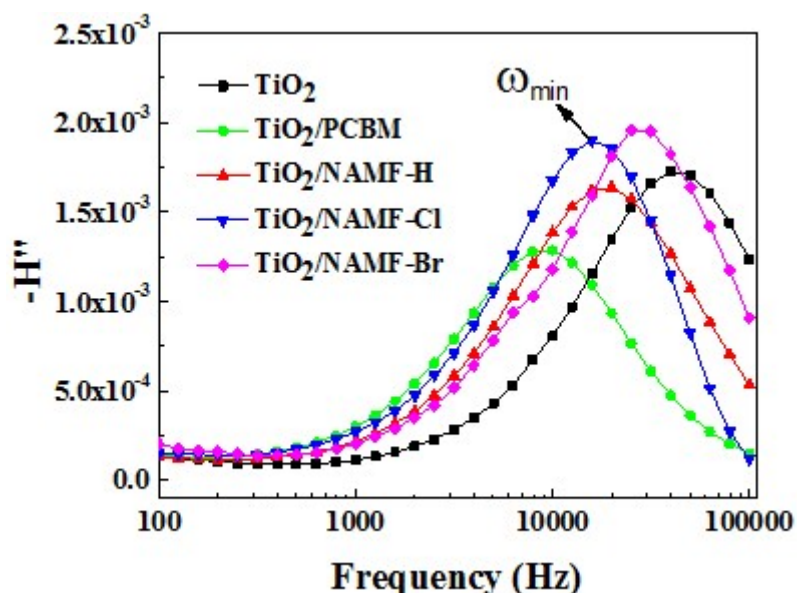


**Figure S11.** IMVS measurements of PSCs with and without fullerene derivative interlayers.